Supplementary Information

Division plane placement in pleomorphic archaea is dynamically coupled to cell shape

James C. Walsh[1,2], Christopher N. Angstmann[3], Alexandre W. Bisson-Filho[4], Ethan C. Garner[4], Iain G. Duggin[2*] and Paul M. G. Curmi[1*]

[1]School of Physics, University of New South Wales, Sydney NSW 2052, Australia.

[2]The ithree institute, University of Technology, Sydney NSW 2007, Australia.

[3]School of Mathematics and Statistics, University of New South Wales, Sydney NSW 2052, Australia.

[4]Molecular and Cellular Biology, Harvard University, Cambridge, MA 02138, USA.

*Corresponding Authors

E-mail: p.curmi@unsw.edu.au (PC); Iain.Duggin@uts.edu.au (ID)

DNA within H. volcanii cells is uniformly distributed.

In *E. coli,* a strong spatial anti-correlation between the division ring and nucleoid distributions in both wild-type and deformed cells has been observed, with the division ring having essentially the same width as the gap between the separated nucleoids (1). From these observations, it has been concluded that positioning of the nucleoids is strongly coupled to the localization of the divisome in *E. coli*, especially in deformed cells (1).

Previous observations of fluorescently stained DNA in *H. volcanii* have shown that DNA fills the majority of the cell volume (2) (compare phase-contrast image, Fig. S1*A*, with DNA staining, Fig. S1*C*). However, cells are not expected to be perfectly uniform in thickness and in particular are thinner at the edges. As a result, the fluorescent signal from the labeled DNA decreases near the cell edge. To test whether the nucleoids in *H. volcanii* are localized or in any way spatially ordered, the distribution of DNA was compared to heterologously expressed green fluorescent protein (GFP), which is expected to be homogeneous throughout the cytosol, to search for any large-scale spatial structure or nucleoid organization (Fig. S1).

The cell outlines of 2,286 cells were detected using automated image analysis. The cross-correlation coefficient between the GFP fluorescence (example shown in Fig. S1*B*) and DNA fluorescence (corresponding example shown in Fig. S1*C*) was then calculated within each cell area. The resulting histogram of cross-correlations is shown in Fig. S1*D*. The mean cross-correlation value was 0.89 demonstrating that the DNA in *H. volcanii* is linearly correlated to the uniform GFP distribution throughout the cell.

To examine large scale deviations between the DNA and GFP distributions, a Gaussian filter with width of 3 pixels (180 nm) was applied to remove local fluctuations resulting from noise. Large scale deviations from the homogeneous state (those remaining after the 3-pixel Gaussian filter) were small in amplitude, with the average maximum difference in each cell of 23.5% between the approximately homogeneous GFP distribution and the DNA. Large deviations tended to occur near the edge of the cell. The maximum deviation occurred on average 280 nm from the edge. Of the pixels that displayed a deviation greater than 20% (4.1% of all pixels), the majority (89.8%) were near to the edge of the cell (within 500 nm). On average, there is slightly less DNA near the edge of the cell, with 2.6% less DNA signal occurring within 500 nm of the cell edge in comparison to the GFP.

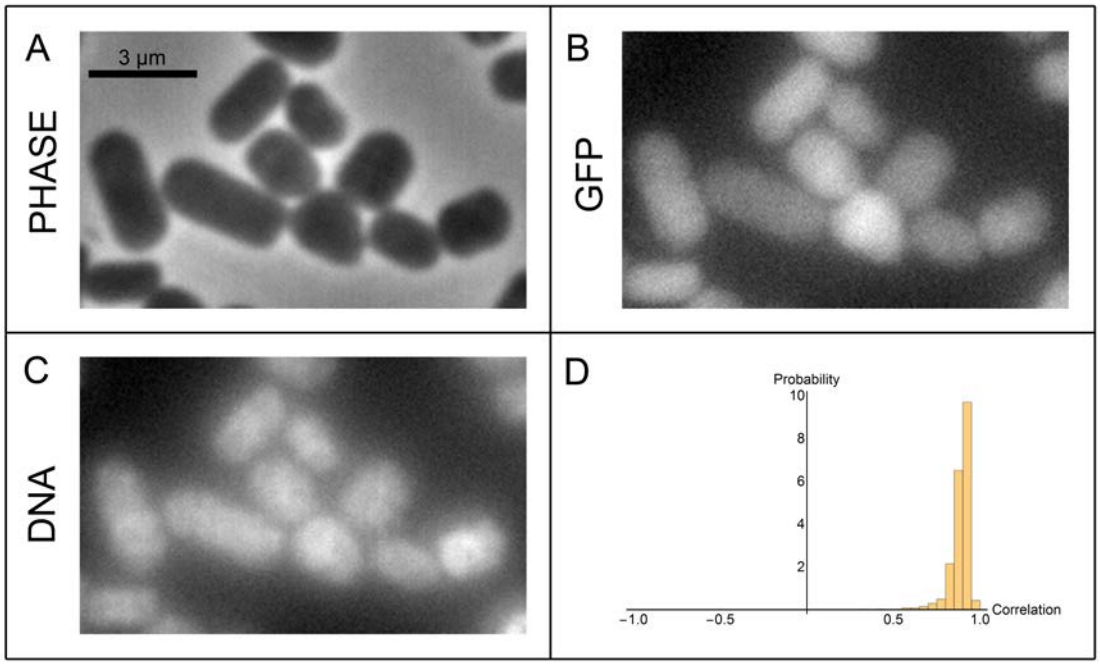

Fig. S1. The distribution of DNA within cells. (**A**) A sample phase-contrast image of *H. volcanii* (H98 + pIDJL40), expressing GFP under the control of a tryptophan-inducible promoter and DNA labeled using Hoechst 33342 DNA stain. (**B**) The corresponding GFP fluorescence image, showing GFP homogeneously distributed throughout the cells. (**C**) The corresponding Hoechst fluorescence image. While a higher level of local variability is apparent in the fluorescence signal compared to GFP, the DNA is nearly homogenous throughout the cell. (**D**) The histogram of the cross-correlation between the GFP and Hoechst distributions from 2,286 cells calculated using automated image analysis. This histogram has a mean of 0.89 confirming quantitatively that the DNA in *H. volcanii* is distributed almost uniformly throughout the cell.

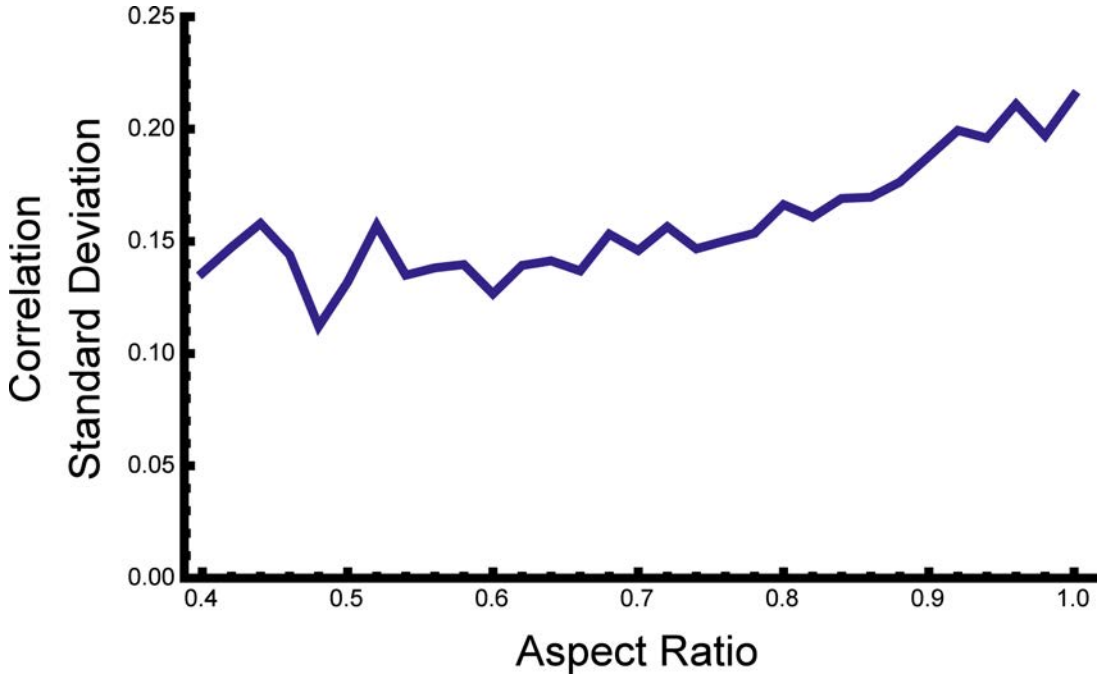

Fig. S2. Standard deviation of division plane prediction. The standard deviation of the cross-correlation between the predicted and observed division plane orientation as a function of aspect ratio for WT *H. volcanii* (H98 + pIDJL40-FtsZ1) cells.

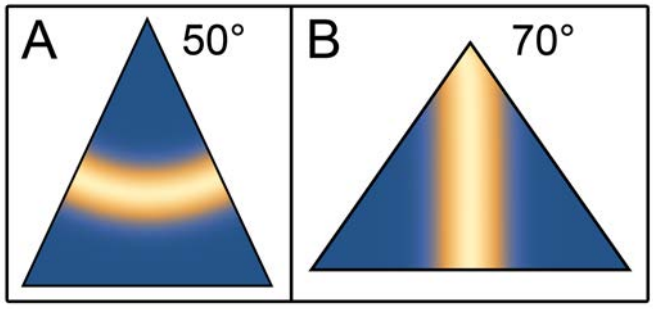

Fig. S3. Bifurcation in the predicted division plane for triangular cells. (**A**) A sub-equilateral isosceles triangle with vertex angle of 50 degrees. The resulting division plane prediction is shown with yellow and blue indicating high and low FtsZ concentration, respectively. This shows the predicted division plane running horizontally, cutting off one corner of the triangle. (**B**) A super-equilateral isosceles triangle with vertex angle of 70 degrees with the resulting prediction This division plane prediction runs vertically from the vertex through the center of the cell, bisecting it.

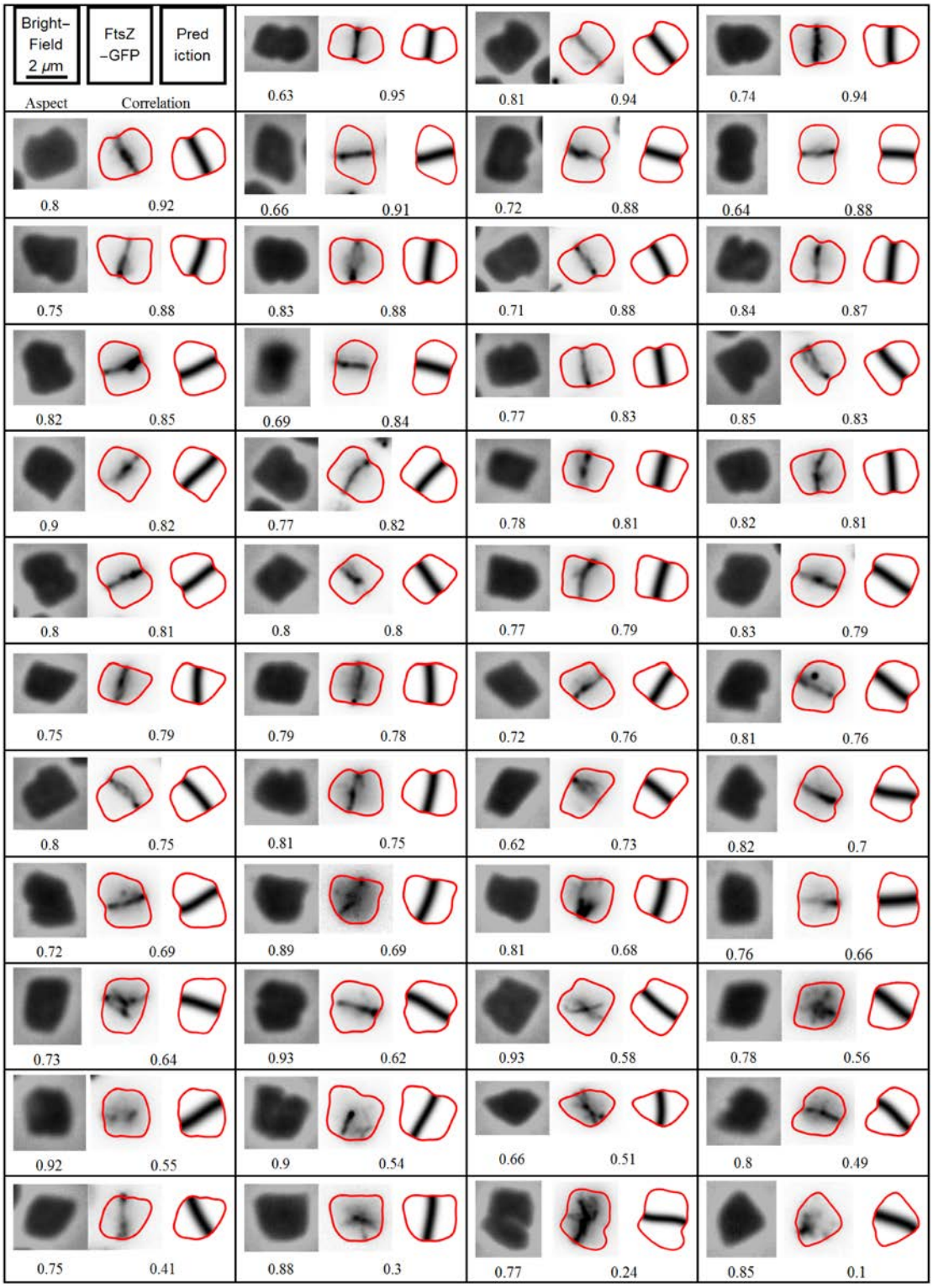

Fig. S4. Experimental cell division orientation in quadrilateral cells. An array showing the division plane orientation in cells of the CetZ1 knockout *H. volcanii* (ID59 + pIDJL40-FtsZ1) that have formed quadrilateral shapes. The left hand number of each panel is the aspect ratio of the cell outline, while the right hand number is the resulting cross-correlation between prediction and observation. The left most image is the phase-contrast micrograph, the middle image is the experimental FtsZ1-GFP fluorescence distribution and the right most image is the predicted division plane.

The cells have been ordered by the cross-correlation between the predicted and observed division planes.

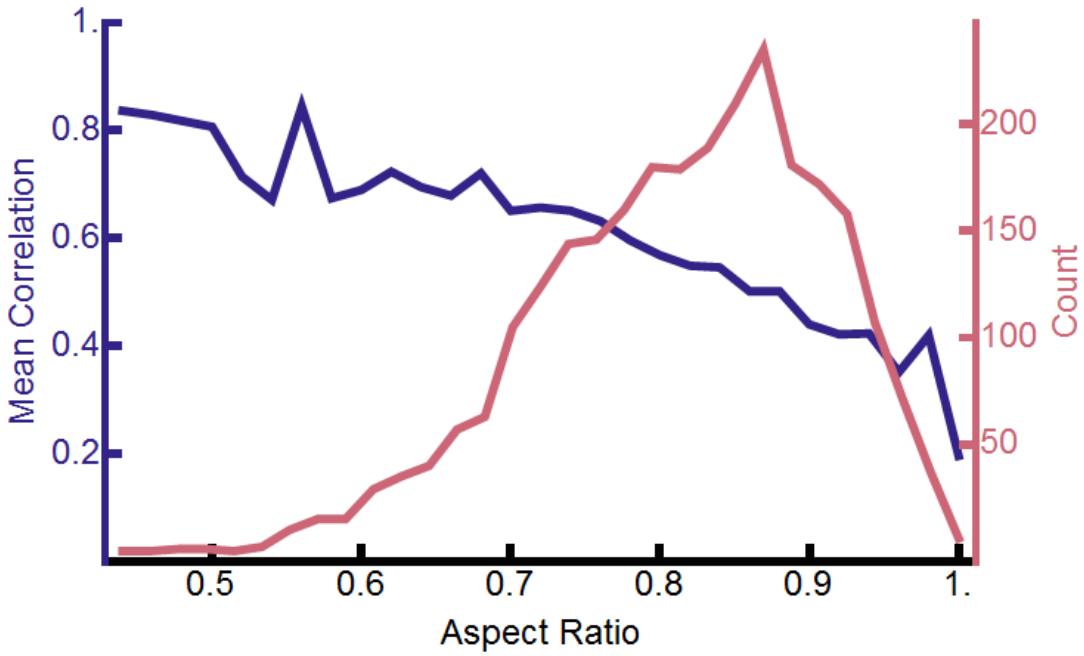

Fig. S5. Division plane prediction as a function of aspect ratio for *H. japonica*. The mean cross-correlation between the predicted and observed division plane orientation for wild type *H. japonica* (TR-1 + pJWID2) cells (solid blue line) as a function of aspect ratio. The density of cells as a function of aspect ratio is shown for wild type cells (solid pink line). 2,672 cell images were used to generate this plot.

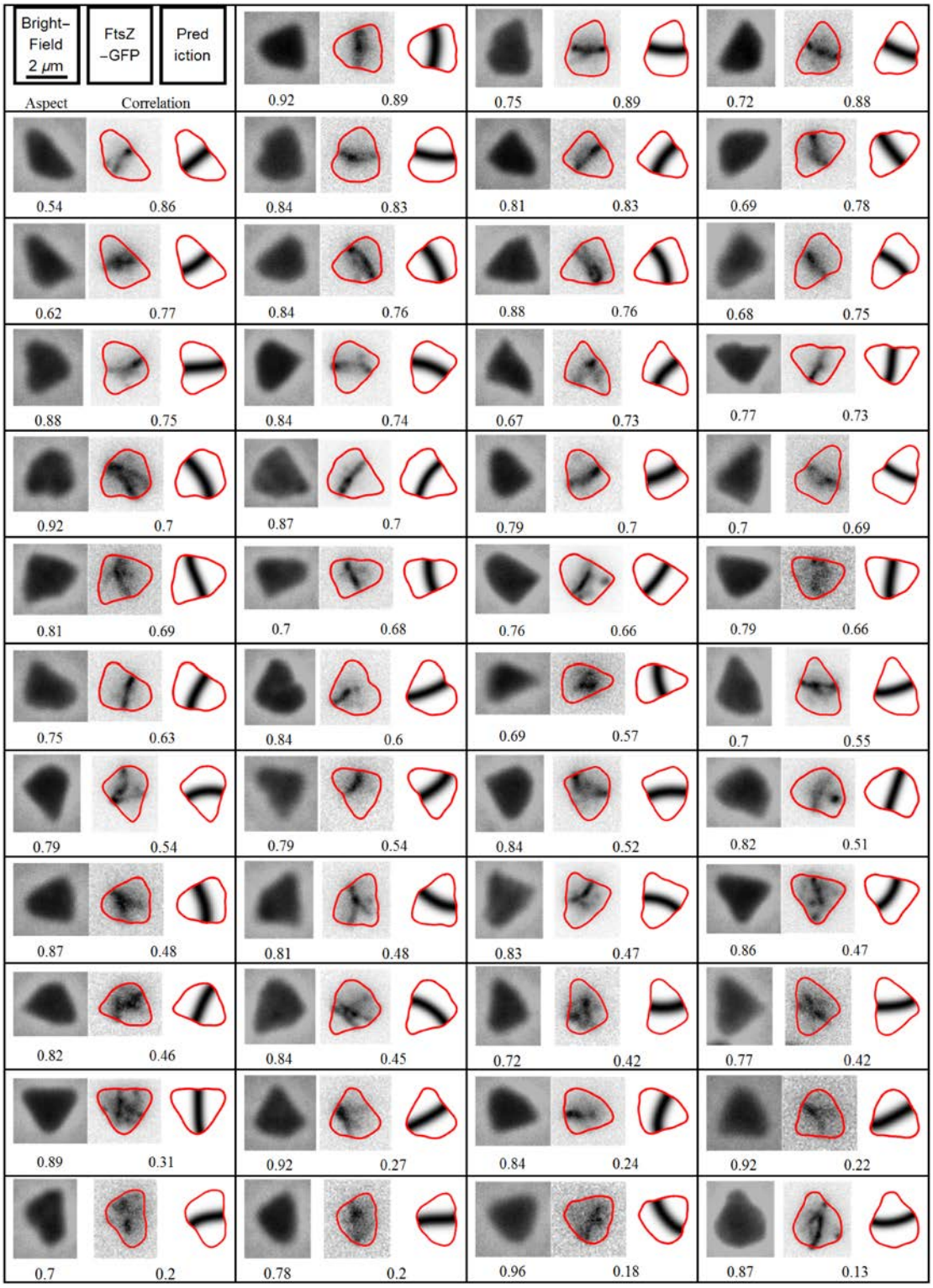

Fig. S6. Experimental cell division orientation in triangular *H. japonica* cells. An array showing the division plane orientation *H. japonica* (TR-1 + pJWID2) cells that have formed triangular shapes. The left hand number of each panel is the aspect ratio of the cell outline, while the right hand number is the resulting cross-correlation between prediction and observation. The left most image is the phase-contrast micrograph, the middle image is the experimental FtsZ-GFP fluorescence distribution and the right most image is the predicted division plane. The cells have been ordered by the cross-correlation between the predicted and observed division planes.

Movies

Movie S1. Four rounds of cell division for *H. volcanii*. The time-lapse movie shows an *H. volcanii* (H98 + pIDJL40-FtsZ1) cell undergoing four rounds of cell division. Left most image: the phase-contrast image with automatically generated cell outlines (yellow); second image: FtsZ1 fluorescence with cell outline; third image: division plane predictions (magenta lines) based on cell shape; and far right image: overlay of FtsZ1 fluorescence and division plane predictions.

Movie S2. Division of an *H. volcanii* cell with near equilateral triangular morphology. The time-lapse movie shows an *H. volcanii* (H26 + pIDJL40-FtsZ1) cell with near equilateral triangular morphology undergoing two rounds of cell division. Left most image: the phase-contrast image with automatically generated cell outlines (yellow); second image: FtsZ1-GFP fluorescence with cell outline; third image: division plane predictions (magenta lines) based on cell shape; and far right image: overlay of FtsZ1 fluorescence and division plane predictions.

References

1. Mannik J, *et al.* (2012) Robustness and accuracy of cell division in Escherichia coli in diverse cell shapes. *Proc Natl Acad Sci U S A* 109(18):6957-6962.
2. Delmas S, Duggin IG, & Allers T (2013) DNA damage induces nucleoid compaction via the Mre11-Rad50 complex in the archaeon Haloferax volcanii. *Mol Microbiol* 87(1):168-179.